

THE N^* PROGRAM AT JEFFERSON LAB - STATUS AND PROSPECTS

VOLKER D. BURKERT

Jefferson Lab, 12000 Jefferson Avenue, Newport News, VA 23606

I discuss recent results on the electroproduction and photoproduction of mesons in the region of non-strange baryon resonances. Results on the quadrupole transition from the ground state nucleon to the Delta show the importance of the nucleon pion cloud. The excitation of the “Roper” $N_{1/2}^+(1440)$ is being studied in single pion production, and the excitation of the lowest negative parity state $N_{1/2}^-(1535)$ is studied in the $p\eta$ and in the $N\pi$ channels. First results on electroproduction of $p\pi^+\pi^-$ show intriguing resonance structure which seems difficult to explain using known baryon resonance properties. Searches for resonances in KY^* and in $p\omega$ channels also reveal resonance-like behavior. I also briefly address a new avenue to pursue N^* physics using exclusive deeply virtual Compton scattering, recently measured for the first time at JLAB and DESY.

1 Introduction

Nucleon physics today is focussed on understanding the details of the nucleon spin and flavor structures at varying distances, and on the systematics of the baryon spectrum. The latter also reveals underlying symmetry properties and internal dynamics.

Resonance electroproduction has rich applications in nucleon structure studies at intermediate and large distances. Resonances play an important role in understanding the spin structure of the nucleon^{1,2} at intermediate and large distances. More than 80% of the helicity-dependent integrated total photoabsorption cross section difference (GDH integral) is a result of the excitation of the $\Delta(1232)$ ^{3,1}. At a $Q^2 = 1\text{GeV}^2$ about 40% of the first moment $\Gamma_1^P(Q^2) = \int_0^1 g_1(x, Q^2) dx$ for the proton is due to contributions of the resonance region at $W < 2\text{GeV}$ ^{4,5}. Conclusions regarding the nucleon spin structure for $Q^2 < 2\text{GeV}^2$ must therefore be regarded with some scepticism if contributions of baryon resonances are not taken into account.

The nucleon’s excitation spectrum has been explored mostly with pion beams. Many states, predicted in the standard quark model, have not been seen in these studies, possibly many of them decouple from the $N\pi$ channel⁶.

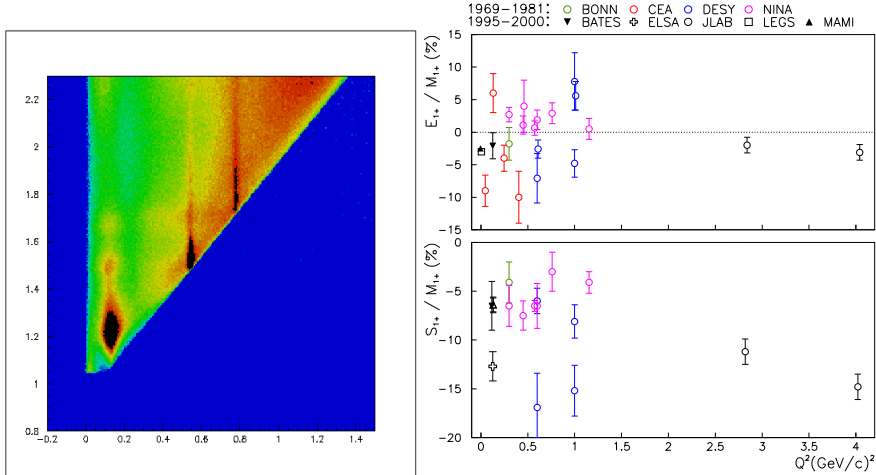


Figure 1. Left: Invariant mass $M_{\gamma^* p}$ versus missing mass M_X measured in CLAS. Right: R_{EM} and R_{SM} before the year 2001

Electromagnetic interaction and measurement of multi-pion final states, may then be the only way to study some of these states. Photoproduction of mesons is being used extensively at LEGS, MAMI, GRAAL, ELSA and JLAB. Electroproduction adds sensitivity due to the fact that the virtual photon carries linear polarization, and due to the possibility of varying the photon virtuality. I will mostly discuss recent results in electroproduction from JLab where accurate data have now become available.

In the past electroexcitation of resonances was not considered a tool of baryon spectroscopy but rather a means of measuring transition formfactors of some prominent states. CLAS is the first full acceptance instrument with sufficient resolution to measure exclusive electroproduction of mesons with the goal of studying the excitation of nucleon resonances in detail. This feature is illustrated in Fig. 1, where the invariant mass W of the hadronic system is plotted versus the missing mass of the $ep \rightarrow epX$, where X represents the undetected system. The π^0 , η , and ω bands are clearly correlated with enhancements in the invariant mass indicating resonances coupling to $p\pi^0$, $p\eta$, and possibly $p\omega$ channels. Some of the lower mass states are already well known. However, their photocouplings and the Q^2 evolution of the transition form factors may be quite uncertain, or completely unknown.

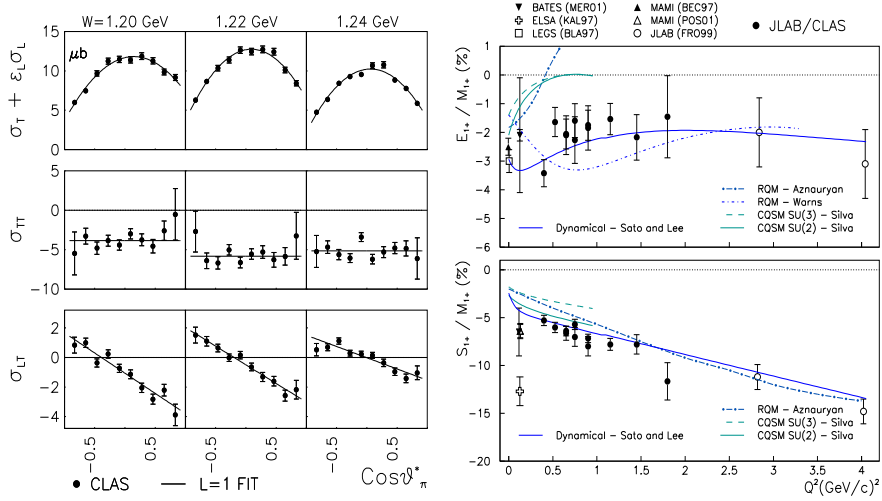


Figure 2. Left: Response functions for $p\pi^0$ in the Delta region. Right: R_{EM} and R_{SM} after 1990, including the latest CLAS results covering the range $Q^2 = 0.4 - 1.8 \text{ GeV}^2$.

2 Quadrupole Deformations of the Nucleon and the Delta

An interesting aspect of nucleon structure at low energies is a possible quadrupole deformation of the nucleon and the $\Delta(1232)$. In the interpretation of ref. ⁸ this would be evident in non-zero values of the quadrupole transition amplitudes E_{1+} and S_{1+} from the nucleon to the $\Delta(1232)$. In models with $SU(6)$ spherical symmetry, this transition is due to a magnetic dipole M_{1+} mediated by a simple spin flip from the $J = \frac{1}{2}$ nucleon ground state to the Delta with $J = \frac{3}{2}$. Non-zero values for E_{1+} would indicate deformation. Dynamically such deformations may arise through interaction of the photon with the pion cloud ^{9,10} or through the one-gluon exchange mechanism ⁶. At asymptotic momentum transfer, a model-independent prediction of helicity conservation requires $R_{EM} \equiv E_{1+}/M_{1+} \rightarrow +1$. An interpretation of R_{EM} in terms of a quadrupole deformation can therefore only be approximately valid at low momentum transfer.

The data for R_{EM} and R_{SM} published before 2001 (Fig. 1) show large systematic discrepancies. Taken together no clear trend is visible. However, at the photon point recent data from MAMI ³ and LEGS ¹² are consistent with a value of $R_{EM} = -0.0275 \pm 0.005$.

The differential cross section for single pion production is given by

$$\frac{d\sigma}{d\Omega_\pi} = \sigma_T + \epsilon_L \sigma_L + \epsilon \sigma_{TT} \cos 2\phi + \sqrt{2\epsilon_L(\epsilon+1)} \sigma_{LT} \cos \phi + h \sqrt{\epsilon_L(1-\epsilon)} \sigma_{LT'} \sin \phi, \quad (1)$$

where ϕ is the azimuthal angle of the pion, and $h=\pm 1$ is the helicity of the incident electron. The response functions σ_i depend on the hadronic invariant mass W , Q^2 , and polar cms pion angle θ_π^* . CLAS allows measurement of the full angular distribution in azimuthal and in polar angle. The former allows separation of the ϕ -dependent and ϕ -independent response functions σ_i at fixed Q^2 , W , and $\cos \theta_\pi^*$, while the latter contains information on the multipolarity of the transition. The multipoles can be extracted in some approximation through a fit of Legendre polynomials to the angular distribution of the various response functions. Angular distributions of response functions at fixed W values are shown in Fig. 2. Results of the multipole analysis are shown in Fig. 2, where data from previous experiments published after 1990 are included as well^{11,13}. R_{EM} remains negative and small throughout the Q^2 range. There are no indications that leading twist pQCD contributions are important as they would result in a rise of $R_{EM} \rightarrow +1$ ¹⁴. R_{SM} behaves quite differently. While it also remains negative, its magnitude is strongly rising with Q^2 . For $Q^2 > 0.35 \text{ GeV}^2$ R_{SM} follows approximately a straight line that may be parametrized as: $R_{SM} = -(0.04 + 0.028 \times Q^2(\text{GeV}^2))$. The comparison with microscopic models, from relativized quark models^{16,18}, chiral quark soliton model¹⁵, and dynamical models^{9,10} show that simultaneous description of both R_{EM} and R_{SM} is achieved by dynamical models that include the nucleon pion cloud, explicitly. This supports the claim that most of the quadrupole strength is due to meson effects which are not included in other models.

The new CLAS data establish a new level of accuracy. However, improvements in statistical precision and the coverage of a larger Q^2 range are expected for the near future, and they must be complemented by a reduction of model dependencies in the analysis. Model dependencies are largely due to our poor knowledge of the non-resonant contributions, which become increasingly important at higher Q^2 . The $\sigma_{LT'}$ response function, a longitudinal/transverse interferences term is especially sensitive to non-resonant contributions if a strong resonance is present. $\sigma_{LT'}$ can be measured using a polarized electron beam in out-of-plane kinematics for the pion. Preliminary data on $\sigma_{LT'}$ from CLAS are shown in Fig. 3 in comparison with dynamical models, clearly showing the model sensitivity to non-resonant contributions. Both models predict nearly the same unpolarized cross sections, however they differ in their handling of non-resonant contributions.

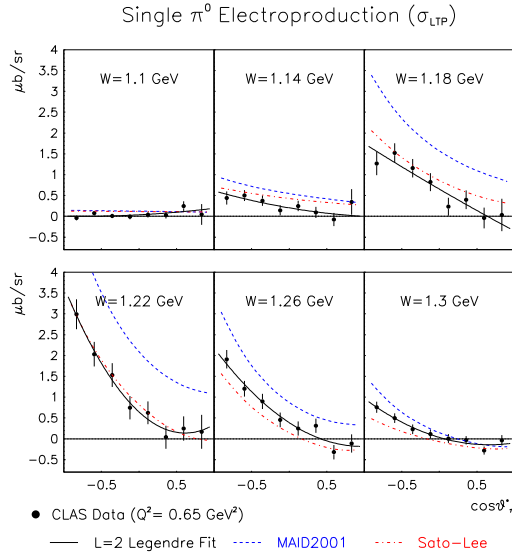


Figure 3. Preliminary $\sigma_{LT'}$ data from CLAS compared to model predictions of Sato-Lee, and MAID2000. Data show strong model sensitivity.

2.1 The $\gamma N \Delta(1232)$ transition in lattice QCD

Ultimately, we need to come to a QCD description of these important nucleon structure quantities. Currently, there is only one calculation in quenched QCD¹⁹ giving $R_{EM} = 0.03 \pm 0.08$, which, due to the large uncertainty, has little bearing on our current understanding of nucleon structure. This calculation was made nearly a decade ago. Improvements in computer performance and improved QCD actions and lattices should allow a reduction of the error to a level where QCD should provide significant input. Such calculations seem feasible now and are part of the program of the Lattice Hadron Physics Collaboration²⁶. They are urgently needed to link these fundamental quantities directly to QCD.

3 N^* 's in the Second Resonance Region

Three states, the elusive “Roper” $N'_{1/2+}(1440)$, and two strong negative parity states, $N^*_{3/2-}(1520)$, and $N^*_{1/2-}(1535)$ make up the second enhancement seen in inclusive electron scattering. All of these states are of special interest to obtain a better understanding of nucleon structure and strong QCD.

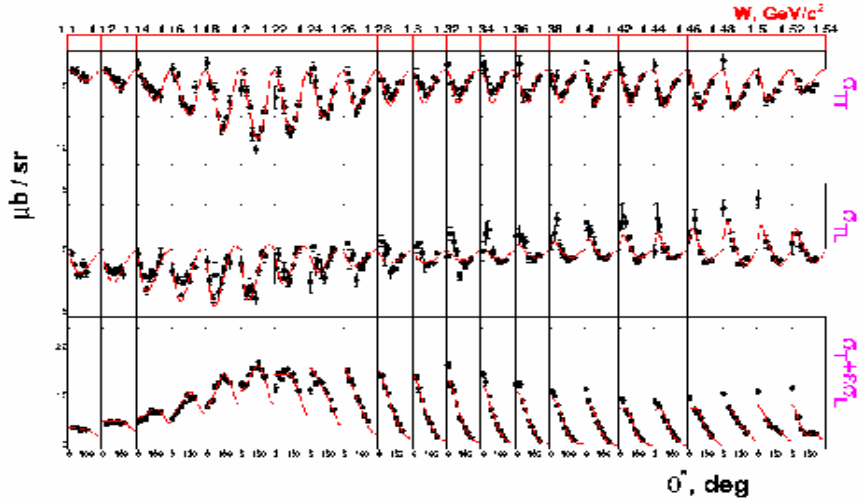


Figure 4. Response functions for $\gamma^* p \rightarrow n\pi^+$. The data cover the $\Delta(1232)$ and the 2nd resonance regions. Angular distributions are shown for each bin in W . The curve represents a fit of a unitary isobar model.

3.1 The Roper resonance - still a mystery

The Roper resonance has been a focus of attention for the last decade, largely due to the inability of the standard constituent quark model to describe basic features such as the mass, photocoupling, and Q^2 evolution of the transition form factors. This has led to alternate approaches where the state is assumed to have a strong gluonic component²¹, a small quark core with a large meson cloud²², or a hadronic molecule of a nucleon and a hypothetical σ meson $|N\sigma\rangle$ ²³. Recent LQCD calculations^{25,26,27} show no sign of a 3-quark state with the quantum numbers of the nucleon in the mass range of the Roper state.

Experimentally, the Roper as a isospin 1/2 state couples more strongly to the $n\pi^+$ channel than to the $p\pi^0$ channel. Lack of data in that channel and lack of polarization data has hampered progress in the past. Fortunately, this situation is changing significantly with the new data from CLAS. For the first time complete angular distributions have been measured for the $n\pi^+$ final state. Preliminary separated response functions obtained with CLAS are shown in Fig. 4. These data, together with the $p\pi^0$ response functions, as well as the spin polarized $\sigma_{LT'}$ response function for both channels have

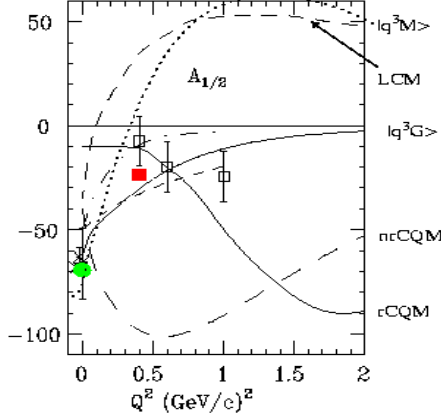


Figure 5. Transverse helicity amplitude $A_{1/2}(Q^2)$ for the Roper resonance. The full squared red symbol is a preliminary point from CLAS (see text). Models include a non-relativistic constituent quark model (nrCQM), relativized model (rCQM), hybrid baryon model ($|q^3G\rangle$), a model in light cone kinematics (LCM), and a model containing a small quark core and meson cloud ($|q^3M\rangle$).

been fitted to a unitary isobar model ³⁰. The results are shown in Fig. 5 together with the sparse data from previous analyses. From all models only the hybrid model ²¹ is somewhat consistent with the measured Q^2 evolution, although much improved data are needed for more definite tests in a large Q^2 range. An important question is if the $A_{1/2}(Q^2)$ amplitude changes sign, or remains negative. Also, all models which assume a 3-quark structure at short distances predict a very slow Q^2 dependence of $A_{1/2}$, while the gluonic model predicts a fast fall-off with Q^2 . The range of model predictions for the Q^2 evolution illustrates dramatically the sensitivity of electroproduction to the internal structure of this state. Model builders should therefore implement electromagnetic couplings and their Q^2 evolution into their models, as experiments can provide most stringent tests.

3.2 The first negative parity state $N_{1/2}^*(1535)$

Another state of interest in the 2nd resonance region is the $N_{1/2}^*(1535)$. This state was found to have an unusually hard transition formfactor, i.e. the Q^2 evolution shows a slow fall-off. This state is often studied in the $p\eta$

channel and shows a strong s-wave resonance near the η -threshold with very little non-resonant background. Older data show some discrepancies as to the total width and photocoupling amplitude. In particular, analysis of $N\pi$ photoproduction data³⁹ disagree with the analyses of the η photoproduction data by a wide margin.

Data from CLAS²⁸, together with data from an earlier JLab experiment²⁹ give now a consistent picture of the Q^2 evolution, confirming the hard formfactor behavior with much improved data quality, as shown in Fig. 6. Analysis of the $n\pi^+$ and $p\pi^0$ data at $Q^2 = 0.4\text{GeV}^2$ gives a value for $A_{1/2}$ consistent with the analysis of the $p\eta$ data at the same Q^2 . Therefore, there is no discrepancy in electroproduction between the $p\eta$ and the $N\pi$ data analyses.

There is also some good news at the theory level. The hard form factor has been difficult to understand in any model. Recent work within a constituent quark model using a hypercentral potential³² has made significant progress in reproducing the $A_{1/2}$ amplitude for the $N_{1/2}^*(1535)$. The hard form factor is also in contrast to models that interpret this state as a $|\bar{K}\Sigma >$ hadronic molecule³³. Although no calculations exist for such models, the extreme “hardness” of the formfactor and the large cross section appear counter intuitive to an interpretation of this state as a bound hadronic system. Lattice QCD calculations also show very clear 3-quark strength for the state^{25,26,27}, making it an unlikely candidate for such a hadronic system.

4 Higher Mass States and Missing Resonances

Approximate $SU(6) \otimes O(3)$ symmetry of the symmetric constituent quark model leads to relationships between the various states. In the single-quark transition model (SQTM) a single quark participates in the interaction. The model predicts transition amplitudes for a large number of states based on only a few measured amplitudes. Electroproduction data for states with masses near 1.7 GeV, many assigned to the $[70, 1^-]$ supermultiplet, are needed for significant tests of this model. Unfortunately, these states decouple largely from the $N\pi$ channel but couple dominantly to the $N\pi\pi$ channel for which no photo- or electroproduction data exist. Moreover, many of the so-called “missing” states are predicted to couple strongly to the $N\pi\pi$ channels³⁶. Study of $\gamma^*p \rightarrow p\pi^+\pi^-$ as well as the other charge channels are therefore important.

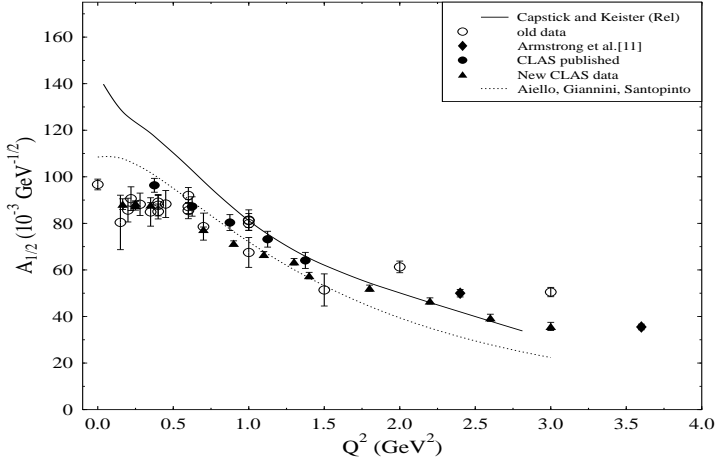


Figure 6. Transverse helicity amplitude $A_{1/2}(Q^2)$ for the first negative parity state $N_{1/2-}^*(1535)$.

4.1 A new $N_{3/2+}^*(1720)$ quark model state?

New CLAS total cross section electroproduction data³⁵ are shown in Fig. 7 in comparison with photoproduction data from DESY. The most striking feature is the strong resonance peak near $W=1.72$ GeV seen for the first time in the electroproduction of the $p\pi^+\pi^-$ channel. This peak is absent in the DESY photoproduction data. The CLAS data³⁵ also contain the complete hadronic angular distributions and $p\pi^+$ and $\pi^+\pi^-$ mass distributions over the full W range. They have been analyzed and the resonance near 1.72GeV was found to be best described by a $N_{3/2+}^*(1720)$ state. While there exists a state with such quantum numbers in this mass range, its hadronic properties were previously found to be very different from the resonance seen in the CLAS data. The PDG gives for the known state a $N\rho$ coupling of $\Gamma_{N\rho}/\Gamma_{tot}(PDG) \approx 0.85$ while the resonance in the CLAS data has a very small coupling to that channel $\Gamma_{N\rho}/\Gamma_{tot}(CLAS) \approx 0.17$. Also, other parameters such as $\Gamma_{\Delta\pi}/\Gamma_{tot} = 0.62 \pm 0.12$ are remarkably different from previous studies of the PDG state. The question arises if the state could be one of the “missing” states. Capstick and Roberts³⁶ predict a second state with these quantum numbers at a mass approximately 1.85GeV. There are also predictions of a hybrid baryon state with these quantum numbers at about the same mass³⁸, although the rather hard form factor as seen in Fig. 7 disfavors such an interpretation²¹. As mass

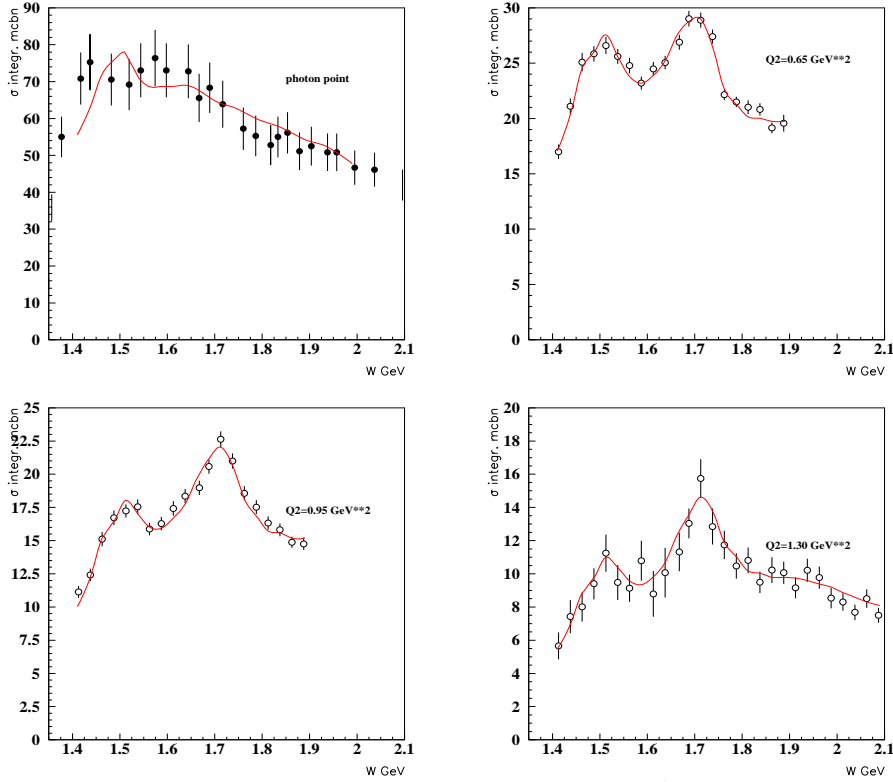


Figure 7. Total photoabsorption cross section for $\gamma^* p \rightarrow p\pi^+\pi^-$. Photoproduction data from DESY - top left panel. The other panels show CLAS electroproduction data at $Q^2 = 0.65, 0.95, 1.3 \text{ GeV}^2$

predictions in these models are uncertain to at least $\pm 100 \text{ MeV}$, interpretation of this state as a “missing” $N_{3/2+}^*$ is a definite possibility. Independent of possible interpretations, the hadronic properties of the state seen in the CLAS data are incompatible with properties of the known state with same quantum numbers as listed in Review of Particle Properties ³⁹. There is no a priori reason why the two states should be identical as the PDG state has been studied in πN scattering, and must therefore couple to πN , while the state seen in the CLAS data only requires coupling to virtual photons and the $N\pi\pi$ channel. More definite conclusions may be drawn when the analysis of single pion electroproduction data in this mass range have been completed.

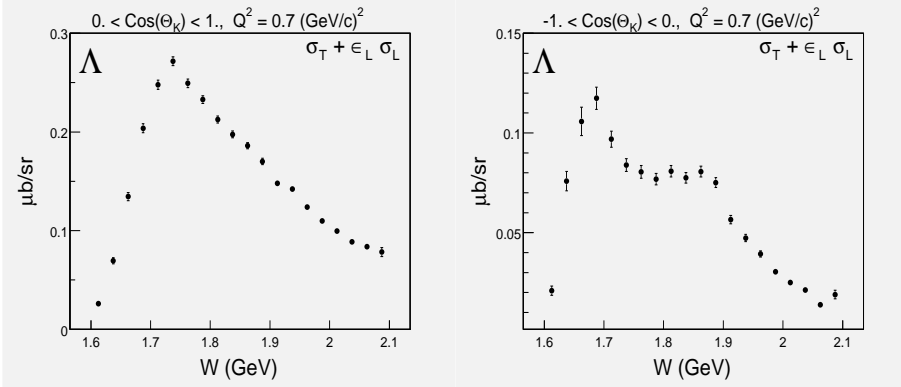


Figure 8. Total photoabsorption cross section measured with CLAS for $\gamma^* p \rightarrow K^+ \Lambda$. The left panel is integrated over the full forward hemisphere in the K^+ angular distribution in the $K^+ \Lambda$ cms. The right panel is integrated over the backward hemisphere.

4.2 Hard nucleon spectroscopy

The isobar analysis of the $p\pi^+\pi^-$ data in Fig. 7 shows that the cross section ratio $R = \text{resonance}/\text{background}$ at $W = 1.72$ GeV is strongly rising with Q^2 . Electron scattering, especially at relatively high photon virtuality, Q^2 , can therefore provide much increased sensitivity in the study of higher mass resonances. Quantitatively, this can be understood within a non-relativistic dynamical quark model ^{40,6}. Photocoupling amplitudes for these states contain polynomials of powers of the photon 3-momentum vector $|\vec{q}|$. For virtual photons the 3-momentum $|\vec{q}|$ for the transition to a given resonances increases with Q^2 leading to the enhancement. In the case of the $N_{3/2}^*$ the non-relativistic quark model predicts (modulo a formfactor which is common to all states) $A_{1/2} = C(|\vec{q}| + |\vec{q}|^3/3\alpha^2)$, where α is the harmonic oscillator constant of the model.

To the degree that non-relativistic kinematics can be applied, spectroscopy of higher mass states with virtual photons at higher photon virtualities (“hard spectroscopy”) has a distinct advantage over the real photon case: as the power n in $|\vec{q}|^n$ depends on the specific $SU(6) \otimes O(3)$ multiplet a state is associated with, it allows enhancing the excitation strength of some states over others by selecting specific Q^2 ranges.

4.3 Nucleon states in $K\Lambda$ production

Strangeness channels have recently been examined in photoproduction as a possible source of information on new baryon states, and candidate states have been discussed^{31,7}. The analysis of the $K\Lambda$ channel is somewhat complicated by the large t-channel exchange contribution producing a peak at forward angles. Preliminary electroproduction data have become available from CLAS⁴¹. To increase sensitivity to s-channel processes the data have been divided into a set for the forward hemisphere and a set for the backward hemisphere. While the cross section in the forward hemisphere shows a t-channel like smooth behavior, clear resonance structures emerge in the invariant hadronic mass for the backward hemisphere (right panel in Fig. 8). The lower mass peak near 1.7 GeV is likely due to known resonances; e.g. the $P_{11}(1710)$, while the peak near 1.85 GeV has no correspondence in the PDG summaries, and maybe associated with the candidate state seen first in the SAPHIR detector³¹ at 1.93 GeV although the mass seems to be considerably lower. A more complete analysis of the angular distribution and of the energy-dependence is needed for more definite conclusions.

4.4 Study of $\gamma p \rightarrow p\eta$

New $p\eta$ photoproduction data from CLAS⁴² cover now the mass range from threshold up to $W = 2.1$ GeV. Nearly complete angular distributions have been measured for all W bins. The total cross section data are shown in Fig. 9. While there is good agreement with previous data from MAMI and GRAAL for $W \gtrsim 1.675$ GeV, there is significant disagreement with the GRAAL data near 1.7 GeV. The sharp rise near the end point of the GRAAL data is not seen in the CLAS data. In the mass range near 1.8 GeV there appears to be significant strength indicating possible resonance excitations. A more complete analysis of the angular distributions and the energy-dependences is needed to come to more definite conclusions regarding resonant strength.

4.5 Resonances in Virtual Compton Scattering

Virtual Compton Scattering, i.e. $\gamma^* p \rightarrow p\gamma$ is yet another tool in the study of excited baryon states. This process has recently been measured in experiment E93-050 in JLAB Hall A⁴³ at backward photon angles. The excitation spectrum exhibits clear resonance excitations in the mass regions of known states, the $\Delta(1232)$, $N^*(1520)$, and $N^*(1680)$. The main advantage of this purely electromagnetic process is the absence of final state interaction, which in meson production complicates the interpretation of the data. A disadvan-

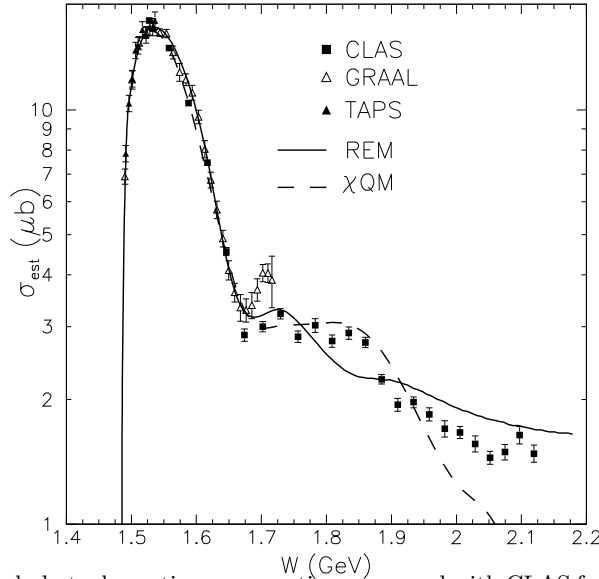


Figure 9. Total photoabsorption cross section measured with CLAS for $\gamma p \rightarrow \eta p$. The curves represent calculations within a Chiral Quark Model and Eta-MAID (REM).

tage is the low rate which makes it difficult to collect sufficient statistics for a full partial wave analysis.

5 Baryon spectroscopy at short distances

Inelastic exclusive virtual Compton scattering in the deep inelastic regime (DVSC) opens up a new avenue of resonance studies at the elementary quark level. The process of interest is $\gamma^* p \rightarrow \gamma N^*(\Delta^*)$ where the virtual photon is deeply virtual ($Q^2 >> 1 \text{ GeV}^2$). The photon couples to an elementary quark with momentum fraction $x + \xi$, which is re-absorbed into the baryonic system with a momentum fraction $x - \xi$, after having emitted a high energy photon. The recoil baryon system may be a ground state proton or an excited state. The elastic exclusive DVCS process has recently been measured with CLAS at JLab⁴⁴ and at DESY⁴⁵ in polarized electron proton scattering, and the results are consistent with predictions from perturbative QCD and the twist expansion for the process computed at the quark-gluon level. The theory is under control for small momentum transfer to the final state baryon. For the inelastic process, where a N^* or Δ resonance is excited, the process can be used to study resonance transitions at the elementary quark level. Varying

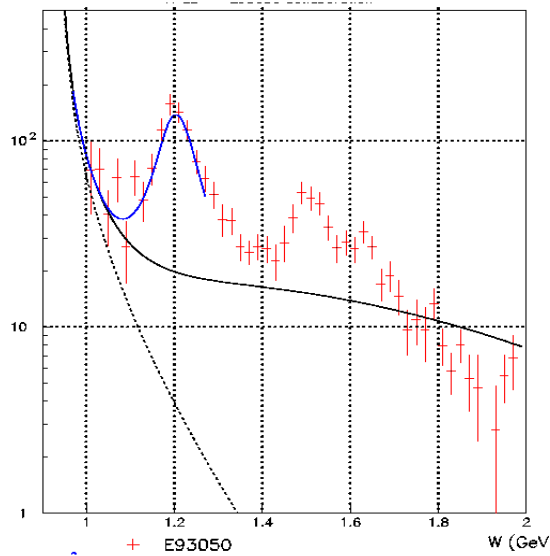


Figure 10. Differential cross section for virtual Compton scattering at $Q^2 = 1$ GeV 2 . The final state photon is in the backward direction relative to the virtual photon .

parameter ξ and the momentum transfer t to the baryonic system, allows probing the correlation functions or generalized parton distributions (GPDs).

That this process is indeed present at a measureable level is shown with the preliminary data from CLAS shown in in Fig. 11. The reaction is measured at invariant masses $W > 2$ GeV. The recoiling baryonic system clearly shows the excitation of resonances, the $\Delta(1232)$, $N^*(1520)$, and $N^*(1680)$. While these are well known states which are also excited in the usual s-channel processes, the DVCS process has the advantage that it decouples the photon virtuality Q^2 from the 4-momentum transfer t to the baryon system. Q^2 must be chosen sufficiently high such that the virtual photon couples to an elementary quark, while the momentum transfer to the nucleon system can be varied independently. In this way, a theoretical framework employing perturbative methods can be used to probe the “soft” NN^* transition, allowing to map out internal parton correlations for this transition.

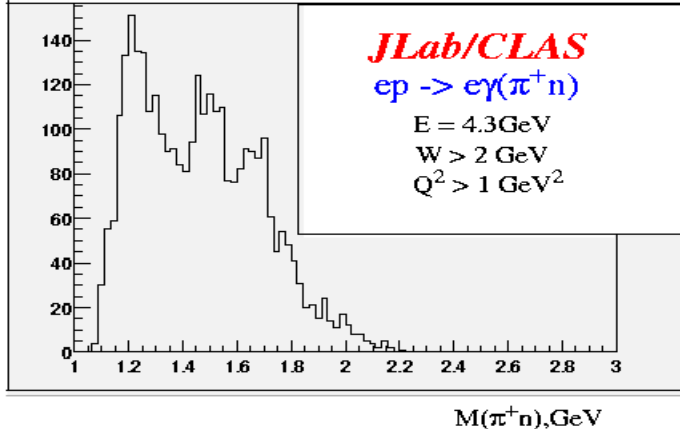


Figure 11. Inelastic deeply virtual Compton scattering measured in CLAS. The recoiling ($n\pi^+$) system shows the excitation of several resonances, the $\Delta(1232)$, $N^*(1520)$, and $N^*(1680)$.

6 Conclusions

Electroexcitation of nucleon resonances has evolved to an effective tool in studying nucleon structure in the regime of strong QCD and confinement. The new data from JLab in the $\Delta_{3/2^+}(1232)$ and $N_{1/2^-}^*(1535)$ regions give a consistent picture of the Q^2 evolution of the transition form factors. Large data sets in different channels including polarization observables will vastly improve the analysis of states such as the “Roper” $N'_{1/2^+}(1440)$, and many other higher mass states. A strong resonance signal near 1.72 GeV, seen with CLAS in the $p\pi^+\pi^-$ channel, exhibits hadronic properties which are incompatible with those of known states in this mass region, and may require introduction of a “missing” baryon state.

While s-channel resonance excitation remains the backbone of the N^* program for years to come, inelastic deeply virtual Compton scattering is a promising new avenue in resonance physics at the elementary parton level, allowing the study of parton correlations within a well defined theoretical framework.

References

1. V.D. Burkert, and Zh. Li, Phys.Rev.D47:46-50,1993
2. V.D. Burkert and B.L. Ioffe, Phys.Lett.B296: 223-226,1992; J.Exp.Theor.Phys.78:619-622,1994
3. J. Ahrens et al., Phys.Rev.Lett.87:022003,2001
4. R. De Vita, Talk at Baryons2002, Jefferson Lab, March 3-8, 2002
5. V.D. Burkert, Nucl.Phys.A699:261-269,2002
6. R. Koniuk and N. Isgur, Phys.Rev.D21:1868,1980
7. A. d'Angelo, Talk at Baryons2002
8. A. Buchmann and E. Henley, Phys.Rev.D65:073017,2002
9. T. Sato and T.S. Lee, T. Sato, this conferences
10. S.S. Kamalov and S.N. Yang, Phys.Rev.Lett.83:4494-4497,1999
11. R. Beck et al., Phys.Rev.C61:035204,2000
12. G. Blanpied et al., Phys.Rev.C64:025203,2001
13. V.V. Frolov et al., Phys.Rev.Lett.82:45-48,1999
14. G. A. Warren, C.E. Carlson, Phys.Rev.D42:3020-3024,1990
15. A. Silva et al., Nucl.Phys.A675:637-657,2000
16. M. Warns, H. Schroder, W. Pfeil, H. Rollnik, Z.Phys.C45:627,1990
17. Z.P. Li, F.E. Close, Phys.Rev.D42:2194-2206,1990
18. I.G. Aznaurian, Z.Phys.A346:297-305,1993
19. D. Leinweber, T. Draper, R.M. Woloshyn, Phys.Rev.D48:2230-2249,1993
20. K. Joo, et al, Phys. Rev. Lett. 88, 122001,2002
21. Z.P. Li, V. Burkert, Zh. Li; Phys.Rev.D46, 70, 1992
22. F. Cano and P. Gonzales, Phys.Lett.B431:270-276,1998
23. O. Krehl, C. Hanhart, S. Krewald, J. Speth, Phys.Rev.C62:025207,2000
24. H. Egiyan, Talk presented at Baryons2002
25. S. Sasaki, T. Blum, S. Ohta Phys.Rev.D65:074503
26. R. Edwards, private communications (2002)
27. W. Melnitchouk et al., hep-lat/0202022
28. R. Thompson et al., Phys.Rev.Lett.86, 1702 (2001); H. Denizli, talk at Baryons2002
29. C.S. Armstrong et al., Phys.Rev.D60:052004,1999
30. I. Aznaurian, private communications (2002)
31. M.Q. Tran et al., Phys.Lett.B445:20-26,1998
32. M.M. Giannini, E. Santopinto, A. Vassallo, Nucl.Phys.A699:308-311,2002; E. Santopinto, private communications (2002)
33. N. Kaiser, P.B. Siegel, W. Weise, Phys.Lett.B362:23-28,1995
34. W.N. Cottingham and I.H. Dunbar, Z.Phys.C2, 41, 1979
35. M. Ripani, Nucl.Phys.A699:270-277,2002
36. S. Capstick and W. Roberts, Phys.Rev.D49:4570-4586,1994
37. V.I. Mokeev, et al., Phys.Atom.Nucl.64:1292-1298,2001

38. S. Capstick, P.R. Page, Phys.Rev.D60:111501,1999
39. D.E. Groom et al., Eur.Phys.J. C15, 1-878, 2000
40. L.A. Copley, G. Karl, E. Obryk, Nucl.Phys.B13:303-319,1969
41. G. Niculescu, R. Feuerbach, private communications.
42. M. Duggar, B. Ritchie, et al., CLAS collaboration (PRL submitted)
43. H. Fonvieille, Talk given at Baryons2002
44. S. Stepanyan et al., Phys.Rev.Lett.87,182002-1(2001)
45. A. Airapetian et al., Phys.Rev.Lett.87, 182001-1(2001)
46. M. Guidal, Talk at this workshop